Sediment and vegetation spatial dynamics facing sea-level rise in microtidal salt marshes: Insights from an ecogeomorphic model

J.-P. Belliard[a,b,*], N. Di Marco[a], L. Carniello[c], M. Toffolon[a]

[a] *University of Trento, Department of Civil, Environmental and Mechanical Engineering, via Mesiano 77, 38123 Trento, Italy*
[b] *Queen Mary, University of London, School of Geography, Mile End Road, E1 4NS, London, United Kingdom*
[c] *University of Padova, Department of Civil, Environmental and Architectural Engineering, via Marzolo 9, 35131 Padova, Italy*

Abstract

Modeling efforts have considerably improved our understanding on the chief processes that govern the evolution of salt marshes under climate change. Yet the spatial dynamic response of salt marshes to sea-level rise that results from the interactions between the tidal landforms of interest and the presence of bio-geomorphic features has not been addressed explicitly. Accordingly, we use a modeling framework that integrates the co-evolution of the marsh platform and the embedded tidal networks to study sea-level rise effects on spatial sediment and vegetation dynamics in microtidal salt marshes considering different ecological scenarios. The analysis unveils mechanisms that drive spatial variations in sedimentation rates in ways that increase marsh resilience to rising sea-levels. In particular, marsh survival is related to the effectiveness of transport of sediments toward the interior marshland. This study hints at additional dynamics related to the modulation of channel cross-sections affecting sediment advection in the channels and subsequent delivery in the inner marsh, which should be definitely considered in the study of marsh adaptability to sea-level rise and posterior management.

Keywords: sea-level rise, sediment transport, vegetation distribution, tidal hydrodynamics, numerical model

1. Introduction

Salt marshes are complex landforms situated between land and sea. Given their locations, these tidal environments offer sustainable buffer of coastline settlements against storm surges and marine flooding [1, 2]. From an ecological perspective, salt marshes provide rare and unique habitats supporting nursery grounds for fishes and breeding/feeding grounds for birds. They also filter nutrients and pollutants from tidal waters and supply abundant organic matter, thus making these tidal wetlands among the most valuable ecosystems on Earth [e.g. 3]. Simultaneously, salt marshes are among the most exposed ecosystems to climate change and human disturbance [4]. Marshes appear to be degrading in various regions worldwide in response to modern accelerations of sea-level rise (SLR), and this degradation is expected to be further pronounced within the current century [5]. In view of their societal and ecological relevance, it is therefore important to improve our understanding on the chief processes that drive salt marsh evolution, particularly in the face of environmental change, to address issues of conservation.

Observing the effects of SLR on natural systems remains difficult mainly because of the many interacting drivers affecting marsh sustainability, yet mathematical models may help in gaining knowledge on the response of marshes to SLR as they can isolate the latter process as a forcing variable [6, 7]. The first generation of models addressed marsh deposition and accretion processes only along the vertical dimension [e.g. 8, 9, 10]. They are all zero-dimensional (0D), or sometimes called one-dimensional vertical (1DV) models, simulating vertical marsh accumulation in time at a single point assumed to be representative for the whole marsh platform. These point-based models use a mass-balance approach and rely on the fundamental physical interplay whereby deposition rates are governed by duration and frequency of tidal inundation [11]. Despite being conceptual in nature, these models have shown that an increase in the rate of SLR leads to a progressive deepening of the marsh platform until the deposition rate becomes equal to SLR. More recently, additional point models of platform elevation have been developed [e.g. 12, 13, 14, 15, 16, 17]. These 0D (or 1DV) models differ both in the (eco)-geomorphic processes accounted for and in the approaches used to simulate fundamental mechanisms such as sediment deposition. They however indicate that, if the rate of SLR exceeds a threshold value, marshes would submerge beyond depths that would preclude vegetation regrowth [17]. Due to their relatively simplified treatment of hydro- and morphodynamic processes, point models are particularly convenient for modeling applications over broad temporal scales. On the other hand, results should be interpreted as exploratory, providing qualitative and general description of long-term marsh behavior [13].

Platform vertical accretion greatly controls marsh morphological evolution. Yet, morphodynamics of intertidal systems

*Corresponding author at: University of Trento, Department of Civil, Environmental and Mechanical Engineering, via Mesiano 77, 38123 Trento, Italy. Tel.: +39 0461 281978

Email address: jll.belliard@unitn.it (J.-P. Belliard)

are not governed solely by depositional processes on the marsh platform [18]. Interactions between the different tidal landforms in the wetland environment and the presence of biogeomorphic features, i.e., *zonation* and the associated geomorphic patterns, lead to spatially varying deposition rates. For instance, suspended sediment concentrations (SSC) on the marsh platform are observed to decrease with distance from tidal channels [19]. Nonlinearities between vegetation dynamics and marsh surface elevation also induce spatial variations in vegetation-enhanced sedimentation rates [20]. Since sedimentation rates vary as a function of position on the marsh, its response to rising sea level will be also spatially varied [21]. These spatial dynamics are not captured by point models. In this respect, marsh accretion models simulating spatial distribution of sediment fluxes and vegetation characteristics have progressively arisen in the literature. As an example, Mudd et al. [22] have developed a one-dimensional (1D) model that addresses deposition rates and vegetation productivity along a marsh transect bounded by a tidal channel from where sediment exchange takes place in the face of SLR. They found that marshes develop different topographic profiles depending on the type of sedimentation process acting upon the marsh surface. Lately, Da Lio et al. [23] showed that vegetation in salt marshes does not only passively adapts to morphological features prescribed by sediment transport, but also contributes to define the marsh topographic profile. With the help of a 1D model, they further explored the response and resilience of tidal biogeomorphic patterns to variations in the forcings, such as the rate of SLR. However, these 1D models do not consider the evolution of the bordering tidal channels and by extension the tidal network, and so cannot fully capture the spatial variability in sediment exchange with the marsh platform.

Accordingly, recent modeling efforts have focused on the coupled evolution of marsh platforms and the intertwined tidal networks with different degrees of complexity. Using a two-dimensional (2D) numerical model, Kirwan and Murray [18] explicitly addressed the long term co-evolution of the marsh platform grown by vegetation with the embedded tidal networks under various SLR conditions. The model demonstrated that the lowering of the marsh platform in response to SLR is accompanied by an expansion of the tidal networks, turning vegetated marsh surfaces into unvegetated ones. In the model, flow routing across the marsh platform is solved by a Poisson boundary value problem introduced by Rinaldo et al. [24]. In addition, deposition rate is simply proportional to above-ground biomass while SSC is spatially uniform, thus neglecting the influence of tidal channels in distributing sediments. Alternatively, non-spatially averaged 2D models [e.g. 25, 21] simulating long-term marsh ecomorphological changes and the interactions with tidal channel dynamics have been proposed. These models indicate that expansion of tidal networks in response to SLR may deliver extra sediments to the inner marsh platform. Similarly to Kirwan and Murray [18], these models are also based on the simplified Poisson hydrodynamic model, yet they treat implicitly the evolution of tidal networks through relationships describing channel geometry.

Ideally, the spatial dynamics of salt marsh systems can only be grasped by considering all interplays between the different tidal landforms and between the many conflicting dynamic ecogeomorphic processes acting at overlapping spatial scales. Accounting for these complexities that are prevalent in real intertidal systems remains an important task for the next generation of salt marsh models [e.g. 7]. Here we use a recently developed modeling framework to study marsh spatial dynamics in the face of SLR [26]. The model explicitly simulates the co-evolution of the marsh platform ecogeomorphology with the embedded tidal networks. Tidal flows and sediment transport are simulated on the basis of detailed hydro- and morphodynamic descriptions and are coupled with vegetation growth and related ecogeomorphic processes which are modeled through process-based equations.

With the help of this ecogeomorphic model, we conduct a conceptual study on the influence of SLR on spatial variations in sedimentation in microtidal salt marshes which are known to be the most vulnerable to changing sea-level [27, 28], and considering different ecological scenarios. In particular, we intend to shed light on the feedback mechanisms, involving physical and/or biological processes, that can strengthen marsh resilience in the face of SLR and the conditions in which their influence becomes limited.

2. Methods

2.1. Model description

Marsh landscape evolution is studied on the basis of the eco-morphodynamic approach that embraces the interactions and feedbacks between the hydrodynamics and the evolving morphology, driven by the sediment transport and mediated by vegetation growth. The underlying processes are implemented in a 2D modeling framework which was introduced by Belliard et al. [26] and subsequently used to study the effect of sediment supply and initial bathymetry on tidal network ontogeny in progressive marsh accretional context. Accordingly, this ecogeomorphic model will be briefly reviewed here and we refer the reader to the forthcoming references for a full description of the model components and their peculiarities.

The modeling framework comprises a hydrodynamic module originally developed by Defina [29], and specifically designed to study flows in very shallow tidal basins being subject to wetting and drying processes. To deal with complex flows over partially wet areas, a phase averaging procedure is applied during the derivation of the shallow water equations. The hydrodynamic computations are solved by means of a semi-implicit staggered finite element method which is based on the Galerkin variational method. A module describing wind wave generation and propagation was further developed and coupled with the original hydrodynamic module providing the WWTM (Wind Wave Tidal Model) model designed by Carniello et al. [30, 31].

WWTM was then coupled with the STABEM (Sediment Transport And Bed Evolution Model) module developed, calibrated and tested by Carniello et al. [32, 33] that simulates the resuspension, transport and deposition of sediments by

tidal currents and wind waves, offering the possibility to include a two-size class mixture of cohesive and non-cohesive sediments. Sediment transport is described by an advection-dispersion equation; sediment resuspension is evaluated by the Partheniades [34] formula suitably modified to account for the stochasticity in the distribution of both the bed shear stress and its critical value which highly affect resuspension at near-threshold conditions; and the settling of sediments is expressed by the classical Krone [35] formula. Eventually, changes in bed elevation result from the net balance between the erosion and deposition fluxes, and are expressed by the sediment continuity equation for fine sediments. Specifically, these bed level changes are integrated over a tidal cycle and then multiplied by a morphological factor, following a modified tide-averaging approach [36]. This morphological factor, which corresponds to a fixed number of tidal cycle, is computed based on the ratio of the maximum integrated bed level change found in the domain within a tidal cycle to a reference value determined through a sensitivity analysis, making the morphological factor adaptive to the morphodynamics [26].

The last component of the modeling framework comprises the ecological module designed by Belliard et al. [26]. This module simulates the growth of the vegetation through the inclusion of biomass - elevation relationships (see Figure 1) using different mathematical representations [e.g. 25, 20] as well as ecological scenarios (e.g. monospecific vs multi-species plant communities). Vegetation effect on flow and morphology can be then determined through biomass-dependent ecogeomorphic processes. The latter includes the capture of sediments by plant stems based on the approach of Palmer et al. [37], the production of organic sediments following the work of Mudd et al. [22] and the enhanced settling of sediments due to plant drag, all contributing to sediment deposition ultimately. This process-based ecological module is able to correctly reproduces the well-documented feedback linking marsh ecology and marsh geomorphology and simulate realistic spatial distributions of the halophytic vegetation in agreement with field observations.

2.2. Model setup

Numerical experiments were conducted on a hypothetical domain whose dimension, configuration and topography directly stem from the simulations performed by Belliard et al. [26].

The computational domain consists of an unstructured mesh of dimension 600 m $\times$ 400 m divided into triangular elements with a mean size equal to 5 m. The lower and upper edges of the rectangular domain constitute the seaward and landward boundaries respectively. The domain is closed by three boundaries where no-flux conditions are applied, and is open at the seaward boundary where conditions are prescribed for the hydrodynamics and sediment concentration such that the domain refers in this case to a filled tidal basin, a type of basin mostly used in physical and numerical experiments [38].

The initial topography represents a marsh system dissected by tidal networks (Figure 2a). The depth at the mouth of the central network is approximately 1.7 m, taking the mean sea level (MSL) as datum, while the marsh platform elevation ranges from -0.1 m to 0.5 m a.s.l. This initial topography results from 30 years of morphological evolution starting from a shallow unchannelized tidal flat forced by a sediment supply $C = 50$ mg/l and a semi-diurnal sinusoidal tide with an amplitude $H = 0.5$ m (i.e., tidal range $2H = 1$ m), as simulated by Belliard et al. [26]. These boundary conditions are representative of microtidal environments such as the Venice lagoon for which the ecogeomorphic model was designed, and the particular morphology depicted in Figure 2a, characterized by concave-up marsh platforms dissected by leveed channels, is typical of microtidal marshes [39, 22, 40, 41, 42]. This warm-up simulation was performed in a marsh accretional context in which Belliard et al. [26] showed that most of the morphological changes occurred during the first 20 years followed by minor and slow changes over the longer term as marsh elevations migrate asymptotically toward the elevation of the highest tidal level. This 30-year period is thus sufficient to capture the majority of the morphodynamic activity in the system and the resulting topography therefore corresponds to a nearly morphologically stable configuration. Different SLR rates R are then prescribed along the seaward channel bordering the marsh system, i.e., the open boundary, whereas the tidal amplitude and sediment concentration remain unchanged. Only one sedimentological class of fine cohesive sediment is considered, consistent with field observations, and which is assumed to be transported mainly in suspension.

The initial conditions and the three ecological scenarios are set in accordance with Belliard et al. [26]: i) unvegetated marshes (hereinafter referred to no-vegetation scenario); ii) marshes grown by monospecific halophytic species such as *Spartina alterniflora* (vegetation type-1 scenario); and iii) marshes grown by multiple halophytic species (vegetation type-2 scenario). In vegetation type-1 scenario, which is representative of sub-tropical salt marshes, aboveground biomass achieved its maximal production at an optimal elevation corresponding to MSL [12]; vegetation quickly dies back for lower marsh elevations due to increasing hypoxic conditions while plant biomass progressively diminishes for higher elevations due to the reduction in the hydroperiod and frequency of flooding leading to high concentrations of salt in pore waters (Figure 1a). On the contrary, in vegetation type-2 scenario, which is typical of temperate salt marshes, aboveground biomass is assumed to depict its maximal production at an optimum elevation corresponding to the highest tidal level (HT) (Figure 1b), in agreement with field observations of increased plant richness and diversity with marsh elevation [e.g. 43, 41]. To be consistent with the new hydrodynamic forcing, these different biomass distributions in the tidal frame are shifted in time due to the varying MSL.

The present contribution aims to bring further insights into the effect of SLR on salt marsh ecomorphodynamics, and in an attempt to make the results as transparent as possible, only pertinent processes have been retained while others have been treated in simplified ways. For this reason, we only adopt constant rates of SLR. Also, the proposed biomass - elevation relationship assumes that local biomass is in equilibrium with local marsh elevation, in line with the findings from Marani et al. [14]

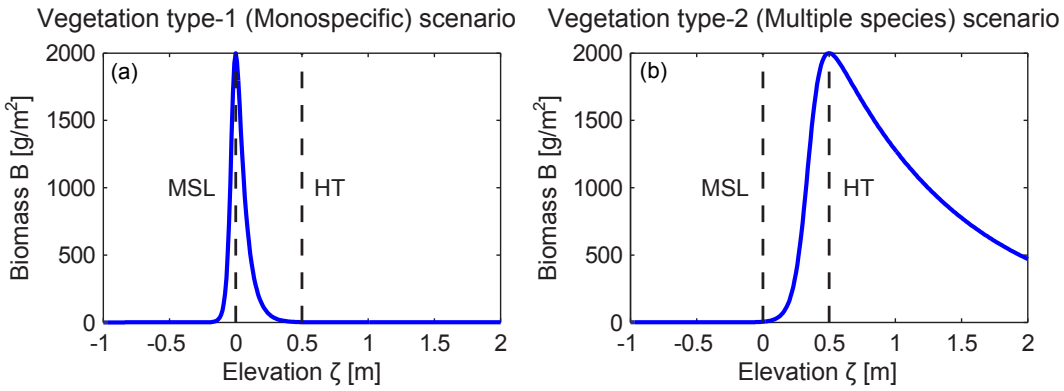

Figure 1: Vegetation biomass density for the two vegetation scenarios; (a) vegetation type-1 scenario; (b) vegetation type-2 scenario (adapted from 26 using 20 formulation); MSL = Mean Sea-Level ; HT = High Tide.

who studied the evolution of marsh biomass and topography by means of an ecogeomorphic model, in which these variables were parameterized using interacting dynamic equations, and observed a quasi-instantaneous biomass adaptation to elevation changes.

The capture of sediment particles by plant stems is expressed by an idealized capture efficiency for which vegetation morphometrics need to be quantified. Mudd et al. [22] determined that these morphometrics followed a power law function of aboveground biomass, on the basis of a long-term record of *Spartina Alterniflora* biomass in North Inlet estuary, South Carolina. To allow a fair comparison between the two ecological scenarios, we assume that this function also holds for marshes characterized by vegetation type-2 scenario, despite such a relationship is likely species specific. Flow resistance due to the presence of vegetation is parameterized by means of an additional friction contribution that represents the drag exerted by plant stems and which we assume to vary linearly with plant biomass [26]. Resulting higher hydraulic roughness triggers a decrease in the depth averaged velocity which in turn leads to a decrease in the bed shear stress, thus enhancing the settling of mineral sediments. The rate of organic sediment production follows the formulation of Mudd et al. [22] that describes a linear relationship between organogenic sedimentation and vegetation biomass on the basis of the pioneered model developed by Randerson [44] and tested against field data.

Wind and wave forcings are neglected in the present set of numerical experiments as we intend to simulate sheltered salt marshes where wind waves are negligible. In truth, from a purely physical aspect, wind-wave erosion can be assumed negligible as the present initial topography contains shallow water depths that typically attenuate the wave-induced bed shear stress [45, 30].

Every simulation is run for a period of 60 years as a trade-off between the high grid resolution needed to capture the morphological features of interest, the fast and detailed scaled variables computed by the model and the resulting computation time. We invite the reader to refer to Belliard et al. [26] for additional details regarding the model setup and parameter settings.

3. Results

In the following, we perform a series of simulations aiming to analyze the response of marsh morphologies to different scenarios of SLR and considering the absence or presence of different types of halophytic vegetation. Results at the global marsh scale are first presented prior to downscaling the analysis to the tidal landforms of interest.

3.1. Changes in marsh scale ecogeomorphology in the face of sea-level rise

We first examine the evolution of the marsh topography (Figure 2) starting from the initial marsh system forced by a SLR rate R = 5 mm/yr, i.e., mean IPCC scenario with SLR projections ~0.5 m by 2100 [46], and grown by multiple halophytic species, i.e., vegetation type-2 scenario, which characterizes the majority of the salt marsh ecology worldwide. The evolution of the marsh morphology is primarily manifested by the increasing elaboration of the tidal networks through headward elongation of the main tidal channels and initiation of lower-order tidal creeks. Progressively, new portions of the marsh platform become flooded and drained by the forming tidal courses, particularly landward (e.g., Figure 2f), which also allows for the transport and delivery of sediments in these low-lying areas, thus raising their elevation. Indeed, the spatial distribution of the highest elevated areas that border the forming tidal courses suggests that tidal and sediment exchanges are primarily taking place with these channels rather than as sheet flow directly from the marsh seaward edge. This hydrodynamics is conformed to flow regimes typically occurring in shallow basins under microtidal conditions [47]. Eventually, by the end of the simulation period (i.e., after 60 years), most of the marsh platform is dissected by tidal networks, allowing for sediment deposition relatively uniformly in the domain (see Figure 2k).

In Figure 3, the final morphology shown in Figure 2k is compared with other simulated morphologies characterized by different scenarios of SLR (rows are distinguished by the different values of SLR rates R, ranging from 0 up to 15 mm/yr in agreement with Rahmstorf's [2007] scenario, i.e., > 1 m by

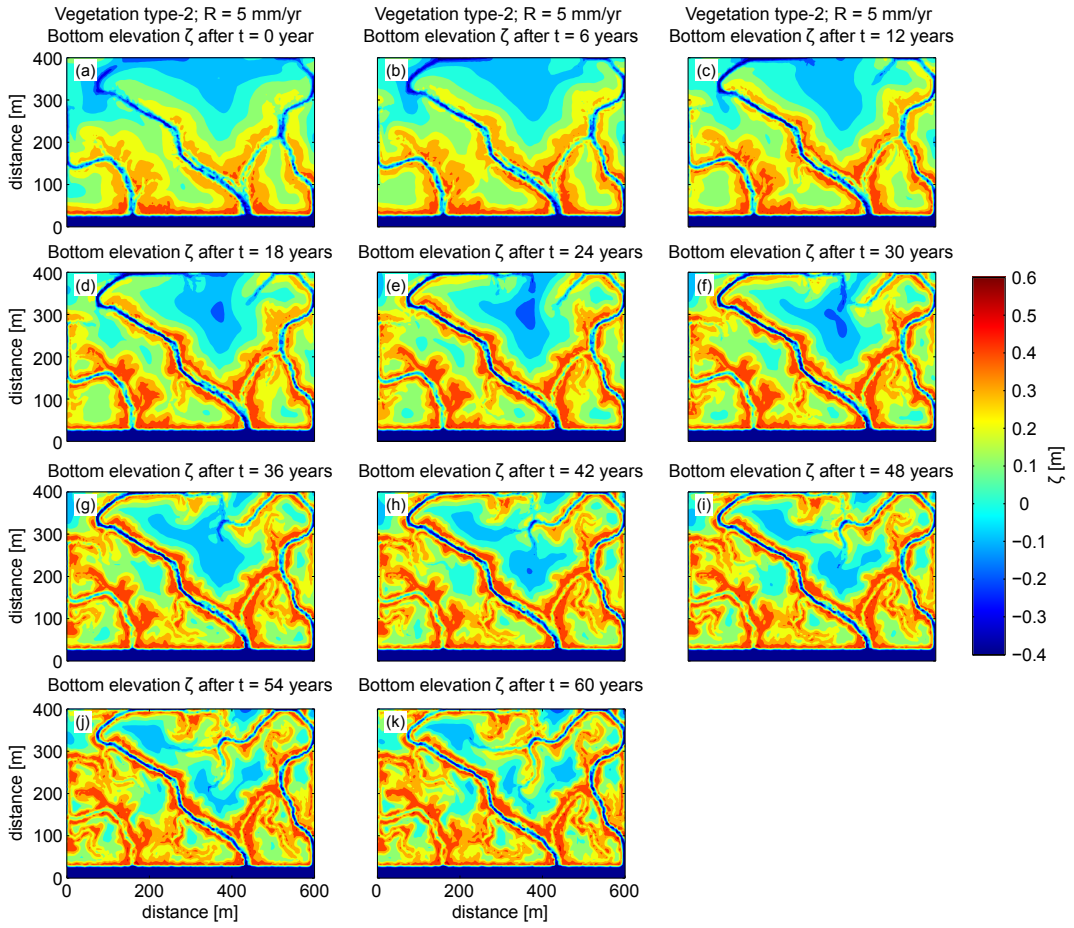

Figure 2: Evolution of the marsh topography characterized by a SLR rate R = 5 mm/yr and vegetation type-2 scenario. Elevation values are relative to the MSL at the time considered. Other forcings are SSC C = 50 mg/l and tidal amplitude H = 0.5 m.

2100) and marsh ecology (columns refer to the scenarios of no-vegetation, vegetation type-1 and type-2 respectively). The diversity in final morphologies as a function of SLR highlights its dominant control on the marsh morphodynamic evolution. What clearly stands out looking at the different planforms is the decrease in marsh surface elevation relative to sea-level with increasing rates of SLR, regardless of the ecological scenarios. This deepening in the tidal frame affects to a greater extent areas of the marsh interior that are more sediment deficient with respect to areas near the tidal channels where the supply of sediments comes from, as also documented in D'Alpaos [21]. This topography agrees with observations in natural microtidal salt marshes like in the Venice lagoon, as shown in Figure 4a.

Vegetation effects on the simulated morphologies however appear less evident in comparison with the SLR forcing. A somewhat lower degree of network elaboration seems characteristic of marshes grown by monospecific halophytic species (i.e. vegetation type-1 scenario) for rates of SLR up to 10 mm/yr (e.g., Figure 3b, e and h), in comparison with the two other ecological scenarios, based on the degree of channel headward elongation. Yet, this morphological change seems to be less obvious for a rate of SLR R = 15 mm/yr (Figure 3k). Conversely, a higher degree of network elaboration is characteristic of morphologies with vegetation type-2 scenario for rates of SLR up to 10 mm/yr (e.g., Figure 3c, f and i), which also becomes less marked for the highest SLR rate (Figure 3l). These distinctions in channel morphology are accompanied with local elevation changes in the regions alongside the tidal channels between the different ecological scenarios.

Therefore, one may question the grounds for these biologically-driven morphological changes which yet seem to cancel out over high rates of SLR. Figure 5 displays the initial biomass spatial distribution together with the biomass difference, namely the biomass after 60 years subtracted by its initial value, for the two vegetation scenarios and rates of SLR considered.

While vegetation type-1 biomass practically disappears after 60 years in absence of SLR, i.e., R = 0 mm/yr (Figure 5c), it survives in portions of the marsh interior with R = 5 mm/yr (Figure 5e). Yet, as R further increases, vegetation type-1 vanishes in these inner marsh areas consequent to the decrease in the corresponding marsh surface relative elevation, as pointed out in Figure 3, which ultimately becomes lower than MSL, i.e., the optimum for biomass productivity for this vegetation scenario (Figure 1a), and so plants die of hypoxia. In truth, vegetation type-1 biomass tends to progressively migrate towards the channel levees where it features narrow vegetation stands surrounding the tidal channels (e.g. Figure 5g and i).

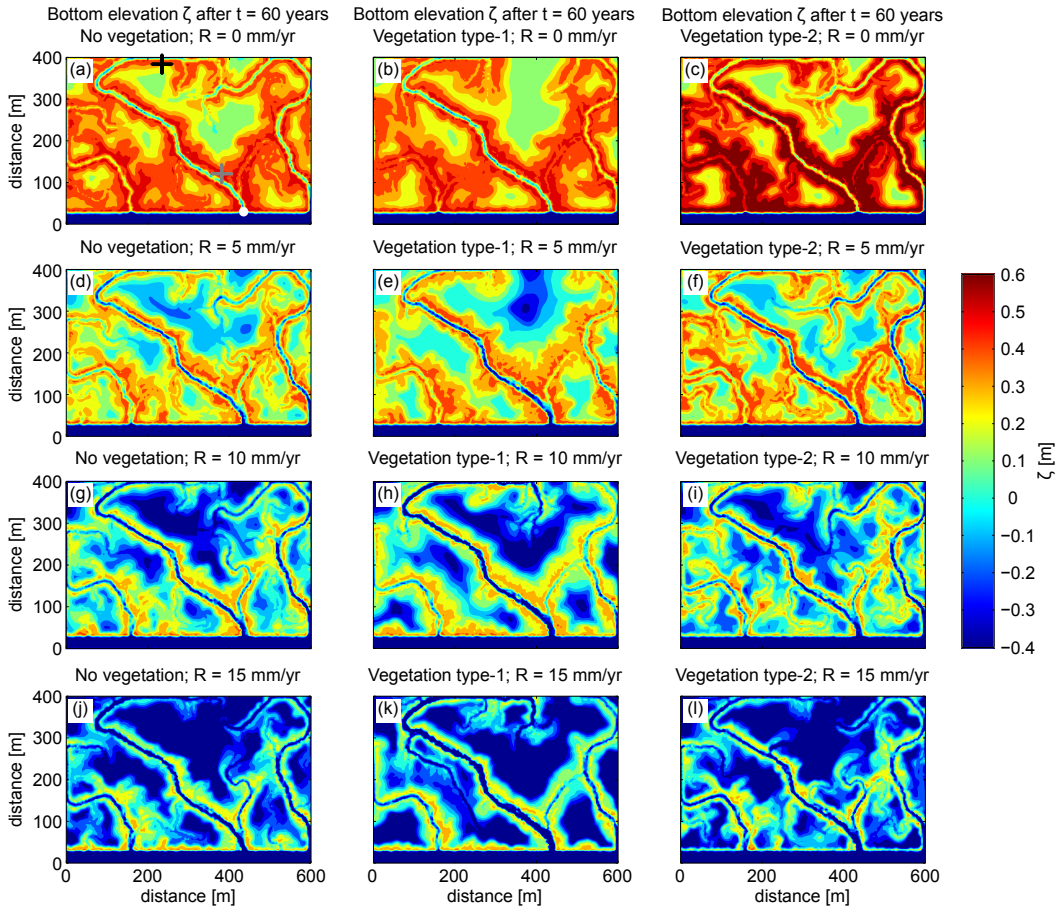

Figure 3: Simulated marsh morphologies after 60 years according to different rates of SLR and marsh ecology. Columns: with different ecological scenarios; rows: with increasing SLR rate R. Elevation values are relative to the MSL at the end of the simulation period (i.e., after 60 years). For every run, C = 50 mg/l and H = 0.5 m. Cross and dot symbols displayed in Figure 3a refer to locations at which variable computations are presented in subsequent Figures.

Indeed, regions near the channels experience more deposition, hence higher elevation (see Figure 3) allowing plants to establish. However, vegetation type-1 can only grow at some distance away from the channel border, namely at locations where the respective marsh surface elevation is approximately equal to MSL, thus illustrating spatially the maximum elevation tolerance above which plants die due to excess of salinity (see Figure 1a).

On the other hand, the highest biomass density under vegetation type-2 scenario is always found in the proximity of the channel levees which is indicative of the positive feedback mechanism linking marsh surface elevation and plant productivity for marshes grown by multiple species. Throughout all SLR scenarios, vegetation type-2 biomass grows primarily landward, alongside the expanding tidal channels, as well as locally with the initiation of low-order tidal creeks. However, this landward biomass growth progressively decreases both in spatial expansion and magnitude as SLR rates increases, to the point where it becomes rather limited for R = 15 mm/yr (see Figure 5j). Concurrently, biomass strongly decreases seaward in the inner marsh platform and remains present only in the channel levees in narrower zonation patterns (compare Figure 5f, h and j). This biomass spatial distribution is consistent with the results of Da Lio et al. [23] as well as with field observations in microtidal salt marshes grown by multiple species (e.g., Venice lagoon), as exposed in Figure 4b.

In an attempt to elucidate this spatial dynamic response of the vegetation in the face of SLR, Figure 6 shows the elevation difference over 60 years for every considered ecological and SLR scenarios. An increase in SLR rate R is associated with an increase in the deposition rate as our model setup involves a constant SSC at the boundary while increasing water levels cause larger water fluxes, thus resulting in higher incoming sediment fluxes. This increase in sediment fluxes can be explained conceptually by the environmental setting considered. As stated previously, our domain intends to reproduce a typical sheltered marsh system located in the innermost areas of a tidal basin such that its seaward limit may correspond to a tidal flat or tidal channel as in the present case. In this particular setting, SLR triggers an increase in water depth which may, in turn, promote sediment resuspension, therefore supporting the assumption of a constant SSC. However, spatially varying sedimentation patterns arise which notably show some dynamics with rising sea-levels. Particularly, the ratio of landward to seaward sedimentation $\Sigma\Delta\zeta_{lw}/\Sigma\Delta\zeta_{sw}$ reduces with increasing scenarios of SLR, noticeable by comparing the spatial expansion

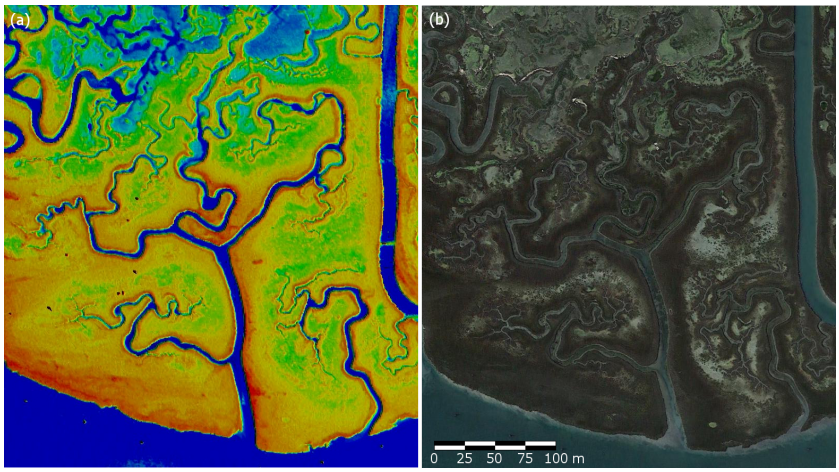

Figure 4: (a) LIDAR-based image showing the topography of a portion of the San Felice salt marsh (Venice Lagoon, Italy). The color sequence goes from higher elevations in red to lower elevations in blue (adapted from 25); (b) aerial photo of the same salt marsh system (courtesy of Andrea D'Alpaos).

and magnitude of the sedimentation patterns between the landward and seaward side of the domain which is schematically delineated by the dashed line in Figure 6. Figure 7 confirms this observation, such that $\Sigma\Delta\zeta_{lw}/\Sigma\Delta\zeta_{sw}$ tends to 1 for R = 15 mm/yr, except for the simulation runs with vegetation type-1 scenario.

Moreover, for a same rate of SLR, vegetation type-2 seems to maintain a higher ratio $\Sigma\Delta\zeta_{lw}/\Sigma\Delta\zeta_{sw}$, especially with respect to the no-vegetation runs (e.g., compare Figure 6d with f as well as Figure 6g with i and compare green with blue line in Figure 7), despite these differences tend to weaken for the highest rate of SLR. Conversely, vegetation type-1 runs show a slightly more pronounced reduction in $\Sigma\Delta\zeta_{lw}/\Sigma\Delta\zeta_{sw}$, as opposed to the two other ecological scenarios (e.g., compare Figure 6e with d and f and compare red line with blue and green lines in Figure 7), until high SLR scenarios where these runs become more effective than vegetation type-2 runs at mitigating the decrease in $\Sigma\Delta\zeta_{lw}/\Sigma\Delta\zeta_{sw}$ (see Figure 7 at R = 15 mm/yr). Moreover, seaward sedimentation alongside the main channels appears to be more confined for vegetation type-2 runs as compared with the two other ecological scenarios, notably vegetation type-l runs (e.g., compare lengths of black arrows in Figure 6g, h and i).

Therefore, the spatial distribution of vegetation and sediments and their dynamics with SLR, illustrated in Figure 5 and 6 respectively, show a certain degree of correlation. For instance, the observed decrease in the ratio of landward to seaward sedimentation $\Sigma\Delta\zeta_{lw}/\Sigma\Delta\zeta_{sw}$ as R increases recalls the landward reduction of biomass growth depicted in Figure 5, primarily for vegetation type-2 scenario. Accordingly, one could attribute this progressive diminution of vegetated areas landward to the reduction in $\Sigma\Delta\zeta_{lw}/\Sigma\Delta\zeta_{sw}$ with increasing SLR. Nevertheless, Figure 6 shows that the latter morphodynamics also occurs for unvegetated marshes, and even to a greater extent. Thus, a closer look on the tidal network landform and its channels, being the "conveyers" of waters and sediments into the system, should be addressed.

3.2. Changes in tidal network characteristics in the face of sea-level rise

Tidal channel hydrodynamics was first examined in order to detect possible differences in the flow field under SLR context. Accordingly, velocity - stage relationships (Figure 8) were quantified at the mouth of the main tidal network common to all simulated morphologies as shown in Figure 3a (white dot). These hydrodynamic variables were computed during a tidal cycle selected at the end of the simulation period. Depth-averaged velocities U refer to the velocity component along the seaward - landward direction and the free surface elevation (stage) η is relative to MSL after 60 years. Highly complex flow patterns emerge in the form of hysteresis loops that are commonly observed for flows in tidal channels [e.g. 49, 50, 51]. In particular, the shape of these hystereses is indicative of the effect of the marsh morphology on the hydrodynamics, manifested by the presence of two velocity transients (surges), of which an example is illustrated by the two black arrows in Figure 8a. Velocity first peaks during the flood just above the bankfull level when a sudden increase in the volume of water is drawn in the channel in order to fill the marsh platform that becomes inundated, whereas the second velocity peak occurs during the ebb just below the bankfull level, thus later within the tidal frame, as previously documented [e.g. 52, 53, 54]. However, regardless of the ecological scenarios, the two velocity peaks arise at a lower stage in the tidal frame with increasing SLR (compare Figure 8a with d). This tendency testifies to the decrease in the marsh surface elevation relative to MSL as R increases, in line with Figure 3, and thus implies a greater proportion of overmarsh tides correspondingly. Therefore, higher and longer overbank flows occur during a tidal cycle. On the other hand, velocity surges are less marked with increasing SLR. Moreover, channel flows are ebb-dominated for R = 0 mm/yr and R = 5 mm/yr, and become approximately balanced for higher R values (e.g., Figure 8d). This sign of tidal symmetry is attributed to the progressive deepening of the marsh platform in the tidal frame with higher SLR rates, thus reducing the effect of the marsh morphology on the hydrodynamics.

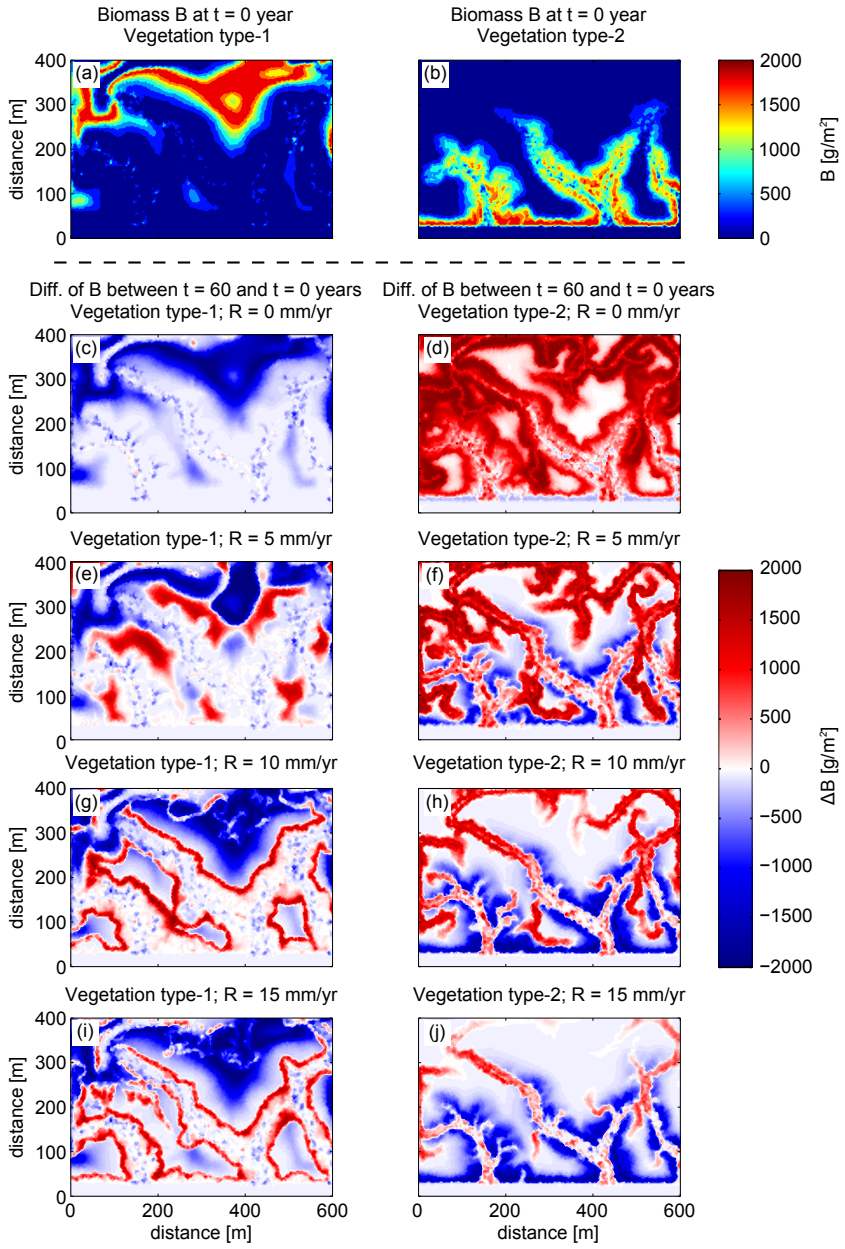

Figure 5: Initial biomass spatial distribution (a,b) and biomass difference (c - j) over 60 years for the two vegetation scenarios (distinguished column-wise) and rates of SLR considered (distinguished row-wise). The biomass difference is computed by subtracting the final biomass distribution based on the morphologies shown in Figure 3 by the initial biomass distribution displayed in Figure 5a and b.

With regard to the comparison between the ecological scenarios, distinctions arise above-all for the vegetation type-1 simulation cases that depict the highest peak flood velocities followed by the no-vegetation and vegetation type-2 cases ultimately, which is evident observing in particular Figure 8b. Therefore, in line with the previous remarks, for a same rate of SLR, overbank flows are particularly significant for vegetation type-1 scenario, and little pronounced for vegetation type-2 scenario. To the opposite, vegetation type-2 scenario exhibits the highest velocity peak during the ebb phase which may allude to a higher drainage contribution in the tidal flow. Note that the little flow reversal occurring during the flood phase in vegetation type-2 scenario in Figure 8c likely results from the drainage of a small shallow basin located near the mouth of the tidal network considered. These differences in flow characteristics between the ecological scenarios however dampen for R = 15 mm/yr. The higher velocity surge detected at the network mouth for vegetation type-1 scenario (see Figure 8b and c) stems from the lower channel density characterizing this scenario (see Figure 3e and h). As little of the marsh interior is dissected by tidal channels, its significant storage capacity triggers an increase in the tidal prism when the water overtops the channel banks in order to flood and drain this area. This lower channel density in presence of vegetation type-1 can be attributed both to the vegetation and sedimentation patterns. Indeed, the inner vegetated marsh basins accrete through bio-physical process which

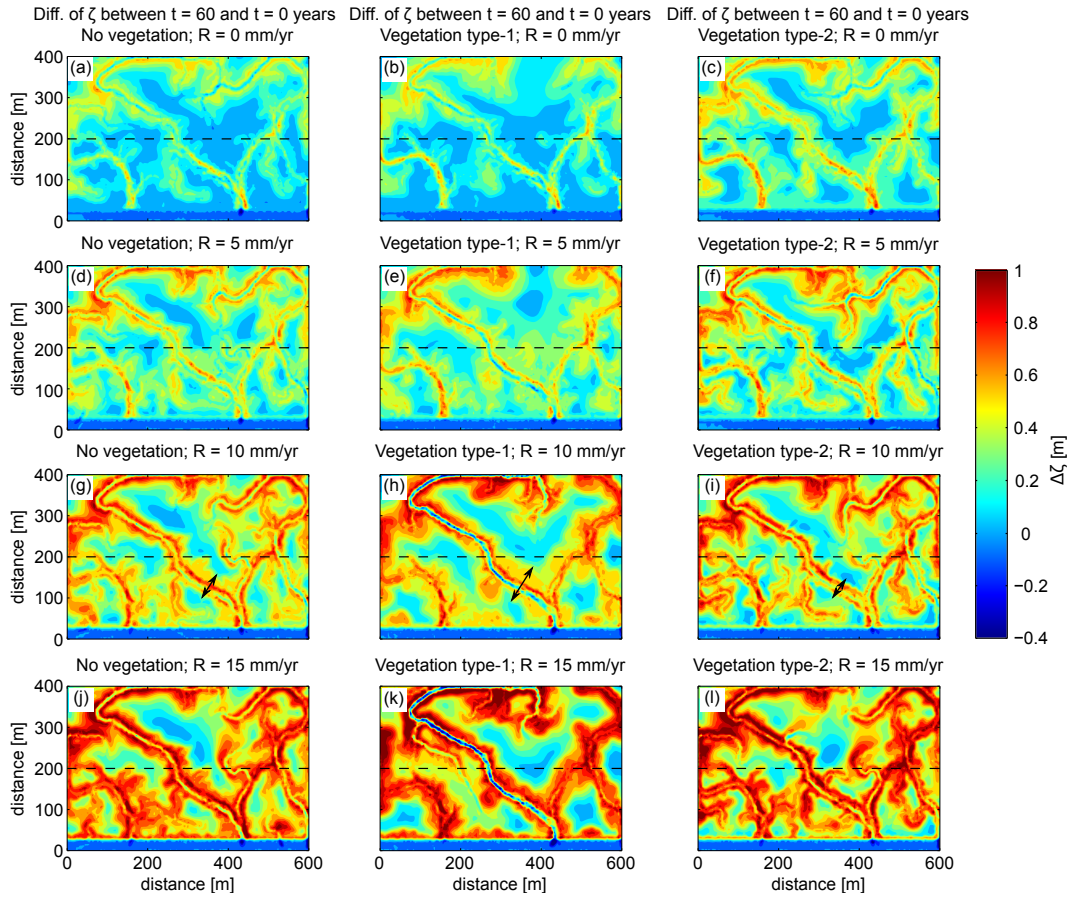

Figure 6: Elevation difference over 60 years for every ecological scenario (distinguished column-wise) and rate of SLR considered (distinguished row-wise). Black arrows illustrate the width of sedimentation patterns developing alongside the highest-order tidal channel of the central network. The dashed line delineates the landward from the seaward part of the tidal basin.

progressively diminishes the topographic relief with respect to the elevated channel levees. Additionally, flow resistance due to the presence of vegetation reduces flow velocities over these basins. As a consequence, the rougher and less perturbed topography guides the sheet flow only to few preferential paths.

Such an intricate tidal channel hydrodynamics bears substantial implications for sediment transport as represented in Figure 9 which exhibits the spatial distribution of the concentration field near high tide. Clear distinctions again emerge on the basis of SLR where SSC in tidal channels progressively reduces landward with rising sea-levels, independently of the ecological scenario. Indeed, tidal networks experience high SSC all over their courses from network mouth to lowest-order channel head for R = 0 mm/yr (Figure 9a, b and c), whereas high concentrations are only present seaward in the highest order channels with R = 15 mm/yr (Figure 9j, k and l). As these spatial distributions of SSC are captured near high tide, this decreasing landward expansion with larger SLR rates suggests that a certain volume of sediments has settled down on the marsh platform priorly during the tidal cycle. This particular dynamics can be explained by the increasing overbank flows with higher R values as highlighted in Figure 8.

Additionally, morphologies grown by vegetation type-2 ensure a more effective landward sediment transport as compared with the two other ecological scenarios. Indeed, since a lower overmarsh tidal incursion characterizes these simulation cases in view of Figure 8, more flows and sediments are constricted in the channels consequently (e.g., compare Figure 9f, with d and e). Conversely, due to the corresponding high overmarsh tidal incursion pointed out in Figure 8, morphologies grown by vegetation type-1 depict on overall the lowest landward concentration extent (e.g., compare Figure 9e, with d and f). The somewhat higher landward extent observed in the central tidal network for the simulation case with vegetation type-1 and under R = 10 mm/yr (Figure 9h) can be ascribed to the higher hydraulic geometries (e.g., channel width) as discerned in Figure 3 which therefore convey more tidal prism, hence more sediment fluxes, with respect to the two other ecological scenarios. These differences in sediment dynamics based on the marsh ecology again vanish for R = 15 mm/yr.

These various hydro and sediment dynamics perform various geomorphological work that are notably captured by the channel levee topographies. Figure 10 displays the evolution of the surface elevation at two points located on a crest of a channel levee in the seaward and landward region respectively, within the same tidal network (see locations of respective cross symbols in Figure 3a), for all the simulated morphologies. Signs of increasing platform flooding with higher SLR rates

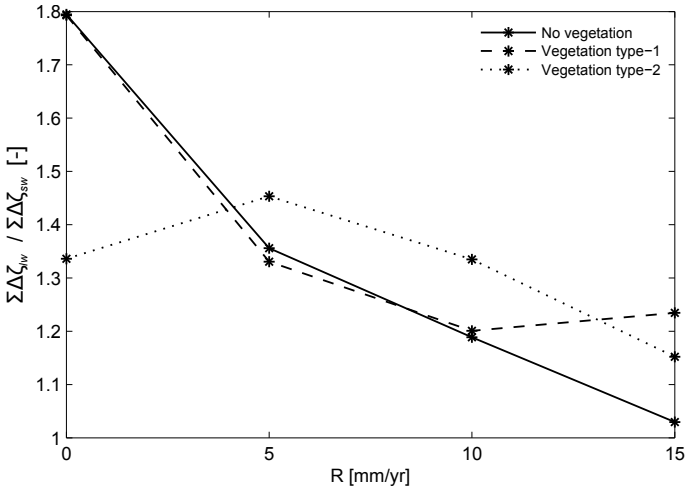

Figure 7: Ratio of landward to seaward sedimentation $\Sigma\Delta\zeta_{lw}/\Sigma\Delta\zeta_{sw}$ for every SLR and ecological scenarios considered.

are again clearly manifested looking at the relative decrease in the levee surface elevation in the tidal frame both seaward and landward with higher R values and regardless of the ecological scenarios. Furthermore, the evolution of the two geographically distinct levee surface topographies reflects the variation in sedimentation rates between the landward and seaward regions driven by SLR as revealed in Figure 6. The 60-year accretion of the landward levee surface slightly increases from R = 5 mm/yr to R = 15 mm/yr whereas its seaward counterpart does so more significantly within the same period (compare individually grey and black lines from Figure 10b-d). Such a behavior provides evidences for the reducing ratio of landward to seaward sedimentation $\Sigma\Delta\zeta_{lw}/\Sigma\Delta\zeta_{sw}$ that occurs with increasing SLR.

Signatures of the vegetation can be distinguished in the evolution of the channel levee topographies. A clear example is given in Figure 10a where the increase in vegetation type-2 biomass as the levee accretes towards high tide enhances ecogeomorphic processes that contribute to further accretion, thereby elevation gain (see dotted grey line in Figure 10a). One can also notice the effect of vegetation biomass, particularly of type-2, in mitigating the decreasing $\Sigma\Delta\zeta_{lw}/\Sigma\Delta\zeta_{sw}$, when comparing the height difference between the seaward and landward levee elevation under vegetation type-2 scenario (e.g., gap between dotted grey and dotted black lines in Figure 10d) with that between the seaward and landward levee elevation under no vegetation scenario towards the end of the simulation period (e.g., gap between continuous grey and continuous black lines in Figure 10d).

4. Discussion

4.1. Conceptual model

Based on the results of this analysis, we propose a conceptual model of marsh spatial ecomorphodynamic response to SLR (Figure 11). This model applies in microtidal regime where salt marshes are initially characterized by a morphology with inner marsh basins embedded by elevated channel levees (see Figure 2a) and tidal flows and sediments are mostly routed via the tidal networks.

Under a relatively low rate of SLR, with R = 5 mm/yr taken here as an example, a significant transport and delivery of suspended sediments take place in the lower marsh interior, as illustrated in Figure 11a. As a matter of fact, the seaward marsh platform experiences limited overmarsh tides due to the relatively high surface elevation of the seaward channel levees in the tidal frame, as shown in Figure 10b. Consequently, small overmarsh tidal prism together with sediment flux are introduced on the flanking marsh platform. On the contrary, a great proportion of the tidal prism at high tide is contained in the tidal network that allows for the landward transport of a large volume of tidal waters and suspended sediments (see Figure 9d, e and f). New portions of the inner marsh become flooded and drained, resulting in higher tidal network expansion (see Figure 2), as previously reported [e.g. 25, 18, 55], which promote, in turn, further sediment settling in these low-lying marshes. Eventually, this series of morphodynamic processes leads to the predominance of landward marsh accretion, as depicted in Figure 6d, e and f.

Dynamics of vegetation productivity influences these spatially-varying sedimentation in response to the imposed low rate of SLR. Specifically, landward accretion is enhanced for marshes grown by multiple species (i.e., vegetation type-2 scenario) by means of two mechanisms. First, the increase in vegetation type-2 biomass landward alongside the developing channels and creeks shown in Figure 5f contributes to higher sedimentation in this region through a set of ecogeomorphic processes namely particle capture, enhanced settling of mineral sediments and organic matter production. Second, the already established high vegetation biomass seaward in the near side of the tidal channels allows levees to further accrete, mainly due to organic sediment production, as revealed in Figure 10b particularly during the first decades. The resulting high elevated channel banks, sketched in Figure 11b, coupled with the added flow resistance provided by the vegetation actively reduce overbank flows (see Figure 8b) and further constrict tidal waters in the channels, as also suggested by D'Alpaos et al. [51]. Accordingly, a more effective landward sediment transport is noticed (see Figure 9f) as well as higher headward extension of the tidal networks (compare Figure 3d with f). Furthermore, the presence of seaward vegetated levees that literally act like "walls" (see Figure 11b) strongly limit channel lateral deposition as the advective and sediment fluxes greatly decrease with distance from the channel edge [19]. Therefore, in the absence of sediments, the seaward backmarsh cannot keep up even with a relatively low rate of SLR and so progressively deepens in the tidal frame, leading to vegetation disturbance (see Figure 4b and Figure 5f).

The net effect of single plant communities such as *Spartina alterniflora* (i.e., vegetation type-1 scenario) on this spatial sediment dynamics appears less evident. The development of vegetation in the inner marshes as depicted in Figure 5e, induces more sedimentation, particularly landward. However, the slightly higher velocity surge detected at the network mouth (see Figure 8b and c) testifies to a somewhat higher overmarsh

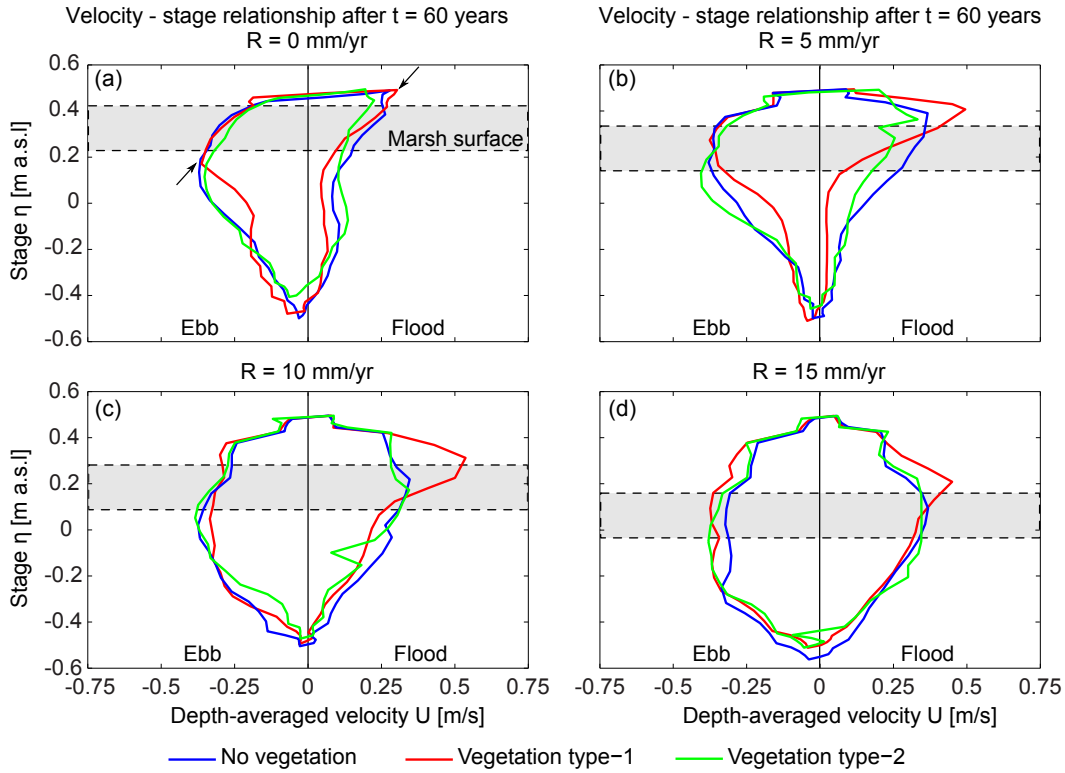

Figure 8: Velocity - stage relationships computed at the mouth of the main tidal network (see white dot location in Figure 3a) after 60 years for every scenario of SLR and marsh ecology. The grey-colored box approximately identifies the marsh surface relative elevation for every applied rate of SLR and whose delineation is based upon the hysteresis profiles for vegetation type-1 scenario where the velocity surges are clearly visible. Stage values are relative to MSL at the end of the simulation period.

tide (i.e., greater overmarsh prism, hydroperiod, inundation depth), as opposed to the two other ecological scenarios. As a consequence, levees in the seaward portion of the channels also accrete, but more laterally than under vegetation type-2 scenario, as the absence of vegetation type-1 biomass on the levee crest allows for sediment to be transported farther from the channel edge. Correspondingly, levees enlarge towards the inner part of the marsh platform (see Figure 11b).

Under a moderate SLR (e.g., R = 10 mm/yr), more overmarsh tidal flow develops seaward due to the lower marsh surface elevation in the tidal frame. As a result, higher hydroperiod, inundation depth and overmarsh prism occur on the marsh platform flanking the channels during the flood which ensure greater sediment flux (see Figure 11c). This increasing platform flooding, also observed in the field [e.g. 40, 56], brings higher sediment deposition seaward, essentially in regions adjacent to tidal channels, and in parallel a reduction of SSC conveyed in the landward marsh interior. Therefore, even if imposing a higher rate of SLR causes higher total accretion rates in the domain (see Figure 6) through the fundamental inundation–sedimentation feedback [7], seaward–landward sediment exchanges yet diminishes and a reduced ratio of landward to seaward sedimentation $\Sigma\Delta\zeta_{lw}/\Sigma\Delta\zeta_{sw}$ is observed as compared with a lower rate of SLR.

Marshes characterized by the multiple species scenario attempt to mitigate this decrease in $\Sigma\Delta\zeta_{lw}/\Sigma\Delta\zeta_{sw}$ through the mechanisms previously described, yet to a lesser extent. As a matter of fact, the building-up of the channel levees consequent to the increasing overtopping allows for plant establishment, which in turn promotes further accretion. However, while the marsh platform heightens in the tidal frame, accommodation space and associated hydroperiod diminish, leading to an asymptotic decrease in the deposition rate towards mean high tide [57]. As marsh morphological adjustments typically lag behind changes in sea-level [58, 6, 59, 17], the marsh platform progressively deepens in the tidal frame while sea-level continues rising, and vegetation biomass declines parallely. Thus, the relative surface elevation of the vegetated levees becomes less significant (see Figure 11d for vegetation type-2), to the point where it becomes even lower than the relative surface elevation of the levees under the two other ecological scenarios after 30 years (see Figure 10c). Owing to this reduced levee height, a lesser volume of sediment migrates and settles down landward, limiting vegetation growth and the related ecogeomorphic feedbacks. The increased platform flooding also perceived for marshes colonized by single species leads to even broaden seaward levees due to the higher overtopping that characterizes this scenario (see Figure 8c) for the reasons explained previously. Thus, more sediment deposition occurs seaward alongside the tidal channels. while the progressive migration of plant colonization towards channel edges contributes to a higher seaward sedimentation too.

Such tendencies are even more pronounced when the system is forced by a high rate of SLR (e.g., R = 15 mm/yr), where

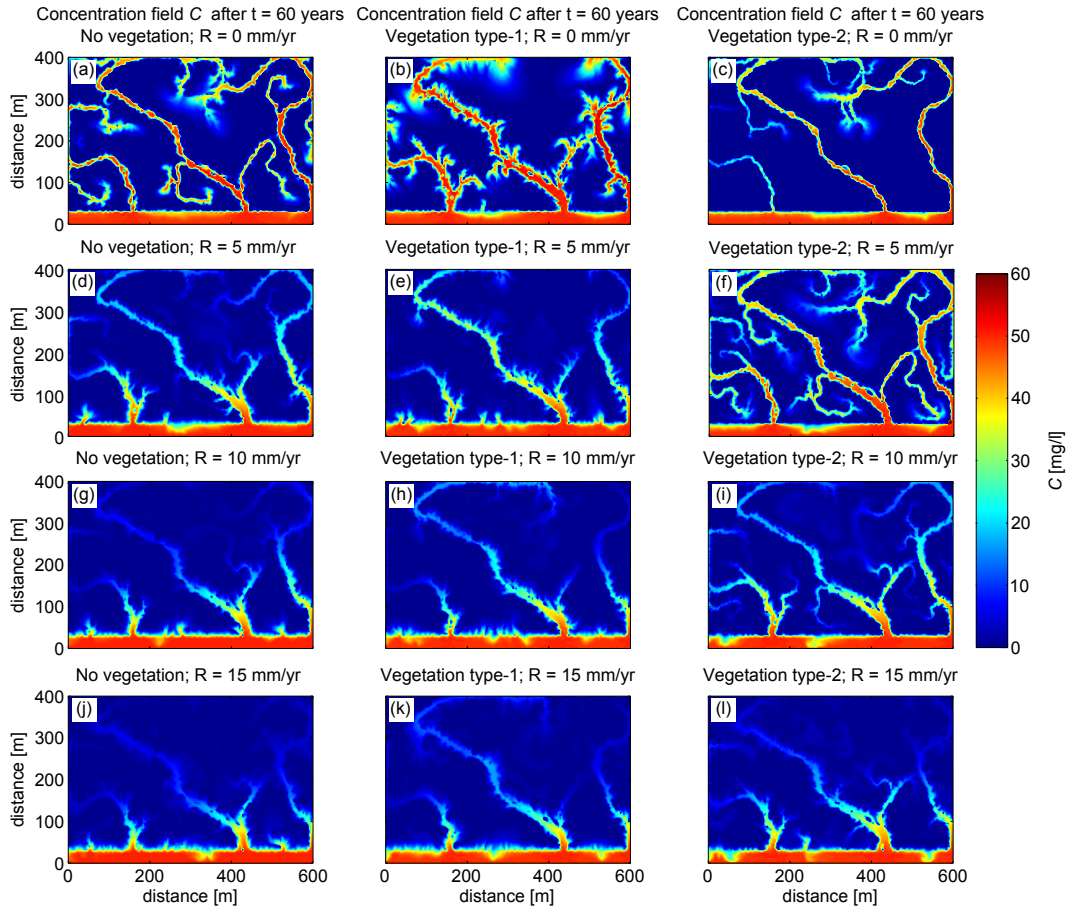

Figure 9: Concentration field near high tide after 60 years for every applied rate of SLR (distinguished row-wise) and ecological scenario (distinguished column-wise).

the progressive prevalence of overmarsh over undermarsh tides (see Figure 8d), as a result of the decrease in the marsh surface elevation relative to MSL, brings about significant sediment deposition seaward. The resulting limited landward sediment transport strongly reduces the delivery of sediments in the lower marsh interior, so much that seaward marsh accretion appear to approximate landward marsh accretion ultimately (see Figure 11e). The effect of the vegetation type-2 in counteracting this decreasing ratio $\Sigma\Delta\zeta_{lw}/\Sigma\Delta\zeta_{sw}$ continues to weaken as the relative marsh height reaches low elevations that limits vegetation growth. The lack of increased biomass density barely sustains levee formation seaward (see Figure 11f) while the consequent strong biomass decline landward inhibits the action of the relevant ecogeomorphic processes in enhancing marsh accretion. Vegetation type-1 biomass similarly declines in the landward region. However, as vegetation type-1 progressively establishes in areas near the channel levees where the local elevation approaches MSL, levee accretion takes place progressively in time as illustrated in Figure 11f. Eventually, this leads to a more effective transport of sediments in the inner marsh to counteract the observed decrease in $\Sigma\Delta\zeta_{lw}/\Sigma\Delta\zeta_{sw}$ (see Figure 7).

4.2. Implications for marsh survival

Having exposed the different ecomorphodynamic processes involved in the marsh dynamic response to SLR, we now examine to what extent these mechanisms can allow the marsh to survive to changing sea-level. Looking at the domain hypsometries may help in this respect (Figure 12). Evidently, an increase in the percentage area of elevation above MSL with respect to that of the initial domain hypsometry is noticed for all morphologies developed under marsh accretional context, i.e., R = 0 mm/yr (see Figure 12a). Under a rate of SLR R = 5 mm/yr, this percentage area is equal to that of the initial hypsometry for the non-vegetation case, and even higher by $\sim$ 8% for the two vegetation cases (compare respective hypsometries at MSL with the help of the dashed lines in Figure 12b). This implies that the simulated marsh morphologies are accreting equal and even faster than the imposed rate of SLR for the two vegetation scenarios. This ability of the marsh to even outweigh rising sea-level is clearly related to the vegetation effects previously described.

However, comparisons between the initial and final hypsometries for higher rates of SLR, i.e., R = 10 mm/yr and R = 15 mm/yr, transcribe a loss of marsh area above MSL of about 20% and 40% respectively (see Figure 12c and d). These observations clearly indicate marsh degradation. Despite local shifts

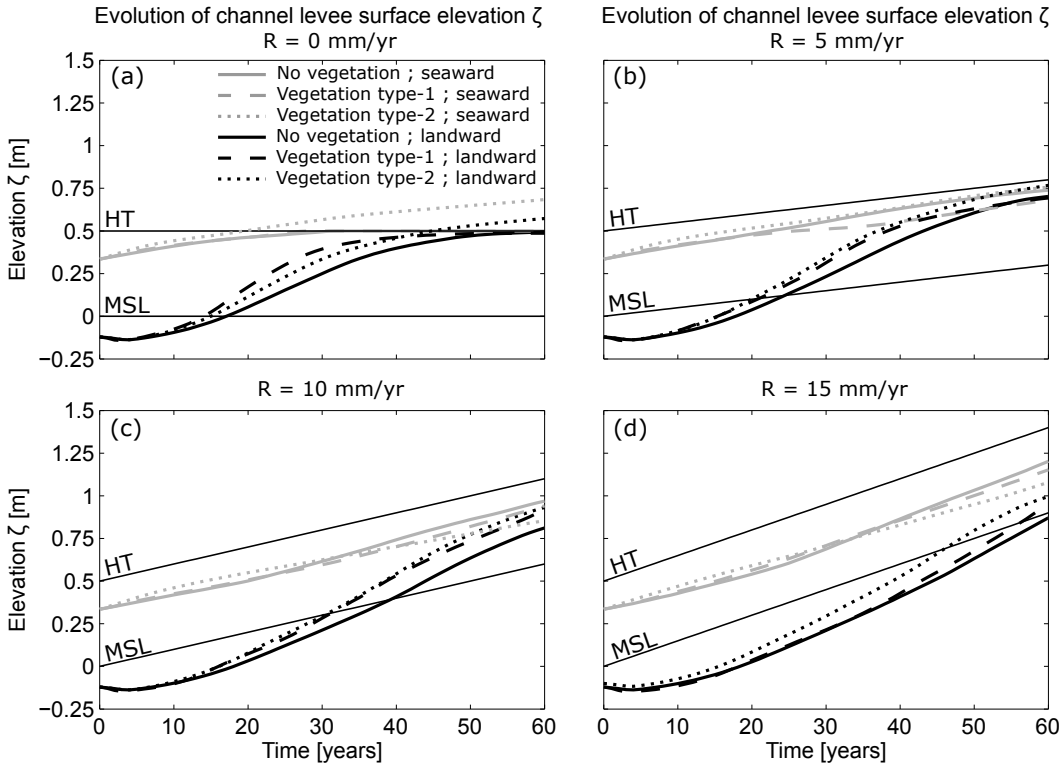

Figure 10: Evolution of the surface elevation measured at two points located on the crest of a channel levee seaward and landward (see locations of black and dark green symbol crosses in Figure 3a) for every considered seal-level rise and ecological scenario. HT: High Tide ; MSL: Mean Sea Level.

in the percentage area, differences between the non-vegetation and vegetation scenarios globally dampen with higher rates of SLR, indicating a reduced influence of the vegetation on the marsh morphology for SLR rates $R > 5$ mm/yr, as pointed out previously. In detail, looking at the final hypsometric curves, marshes grown by single species (vegetation type-1) scenario depict slightly larger areas of surface elevations near MSL (see central black arrows in Figure 12c and d) due to the corresponding maximal biomass productivity featured at MSL (Figure 1a). In contrast, marshes with vegetation type-2 have somewhat larger areas of high surface elevation (see black arrows on the right in Figure 12c and d) due to the increase in biomass productivity with marsh elevation (Figure 1b), as well as smaller areas of low surface elevation (see black arrows on the left in Figure 12c and d) that provide evidences of the enhanced landward accretion particularly marked for this ecological scenario.

To help in confirming these tendencies regarding marsh fate in the face of SLR, Figure 13 displays the time series of the tidal prism, mean accretion rate and vegetated areas for the simulated morphologies. Due to the decrease in the marsh elevation relative to sea-level as distinguished in Figure 3, higher inundation depths occur which result in an increase in the tidal prism with SLR (Figure 13a). In turn, the higher tidal prism is accompanied by an increase in the mean accretion rate over the domain (Figure 13b). However, a closer look shows that, for high SLR scenarios, i.e., $R > 5$ mm/yr, the mean accretion rates never equilibrate the respective rates of SLR throughout the entire simulation period, and regardless of the ecological scenarios (see green and red lines in Figure 13b). On the contrary, for $R = 5$ mm/yr, the corresponding accretion rates are faster than the rate of SLR until they become nearly equal after 60 years (see cyan lines in Figure 13b). This situation whereby accretion balances SLR indicates that marshes forced by a rate of SLR $R = 5$ mm/yr have attained an equilibrium elevation at which the marsh position in the tidal frame remains unchanged [17], as also illustrated in Figure 12b. This equilibrium condition is also manifested looking at the relatively constant tidal prism in time for the three ecological scenarios (see cyan lines Figure 13a) as well as the little change in the percentage of vegetated area in time for the two vegetations scenarios (see cyan lines in Figure 13c) under this moderate rate of SLR. Moreover, the reduction in the percentage of vegetated area that features morphologies forced by SLR rates $R > 5$ mm/yr explains the progressively weakened control of the vegetation on the hydrodynamics, sediment transport and morphology as previously observed throughout this analysis.

Comparing variations in the tidal prism or the mean accretion rate based on the ecological scenarios for a presecribed R value (i.e., lines of same colors) with variations based on the rates of SLR (i.e., lines of different colors) suggests that vegetation control on the marsh morphology appears somewhat secondary. Such a remark invokes the model comparison study of Kirwan et al. [28] where simulations were performed to quantify the threshold rate of SLR for marsh survival under different tidal regimes and sediment supply. Results showed a close match between the five numerical models used in the study despite notable differences regarding both the inclusion and the parameterization of ecogeomorphic processes. Manifestly,

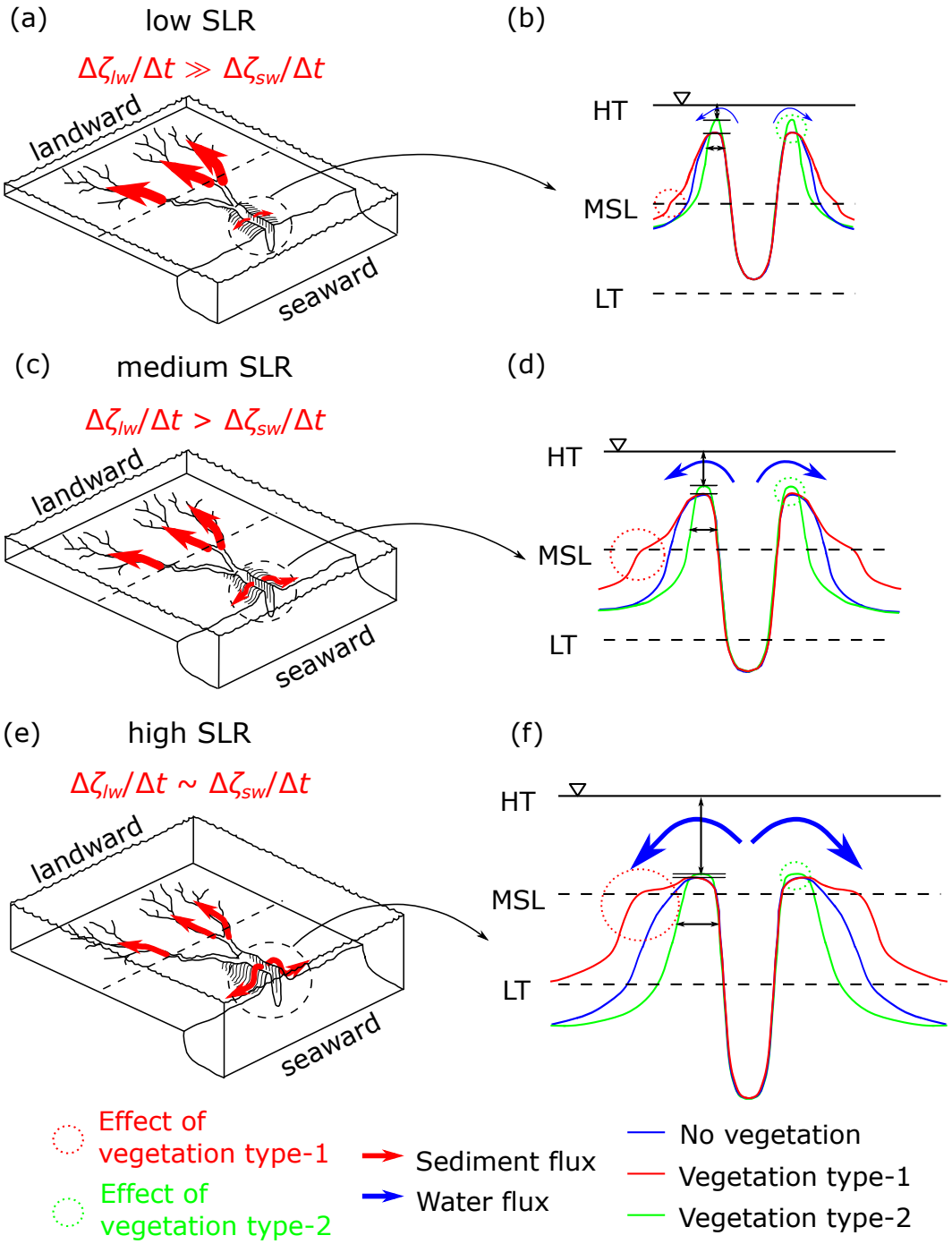

Figure 11: Conceptual model of the spatial ecomorphodynamic response of microtidal marshes to SLR. Left: landscape view illustrating the decreasing ratio of landward to seaward sedimentation $\Sigma\Delta\zeta_{lw}/\Sigma\Delta\zeta_{sw}$ with increasing rates of SLR; right: "zoom in" on seaward channel cross-sections highlighting idealized differences in channel morphology on the basis of the ecological scenarios and the implications in water and sediment transport.

the physical sedimentation - inundation feedback appears to be prevalent in driving the marsh dynamic response to SLR.

Accordingly, while vegetation effect is able to make marshes gain elevation at a rate faster than the rate of SLR for $R = 5$ mm/yr (see Figure 12b), yet it cannot prevent marsh from degradation for higher rates of SLR. Recalling the conceptual model of marsh ecomorphodynamic response to SLR, it seems that the ability for the marsh to keep pace with the rate of SLR is associated with the effectiveness of transport of sediments toward the interior marshland. In other words, the decreasing ratio of landward to seaward sedimentation $\Sigma\Delta\zeta_{lw}/\Sigma\Delta\zeta_{sw}$, triggered by the increase in SLR, precludes the marsh from sur-

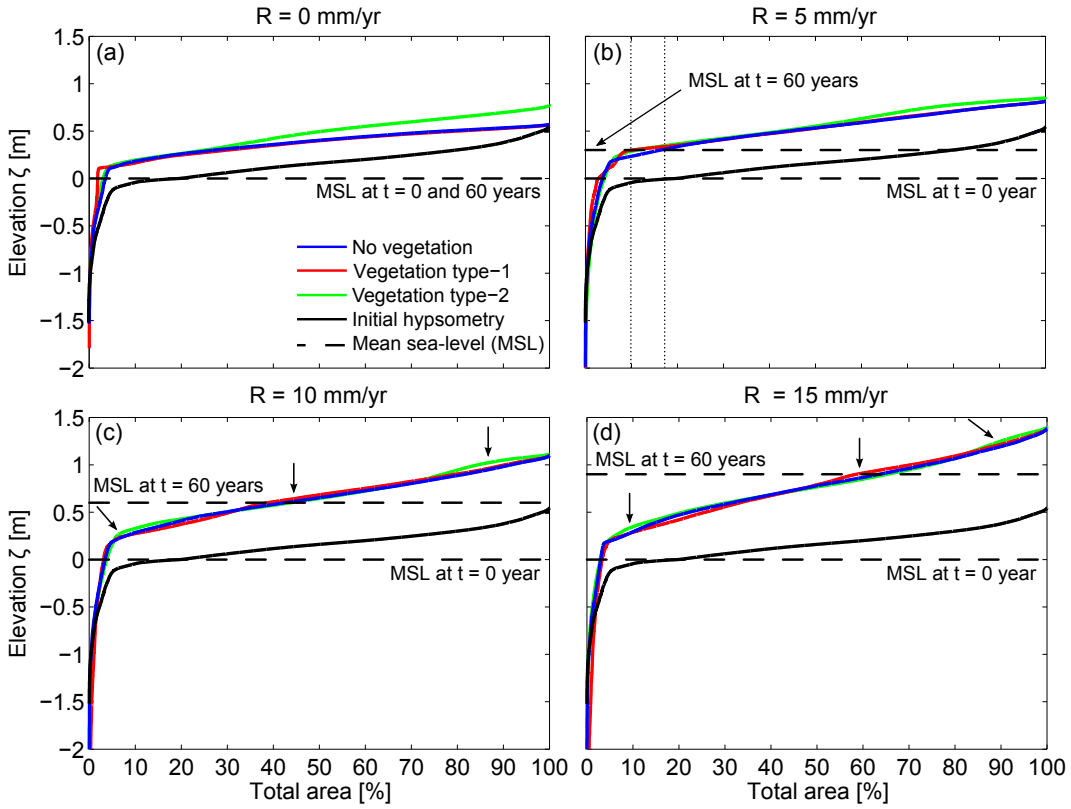

Figure 12: Initial and final domain hypsometries for every SLR rate and ecological scenario. In this case, the bottom elevation corresponds to its absolute value and so is not relative to the MSL after 60 years. The two vertical lines in Figure 12b are marks helping in determining the percentage area that corresponds to a bottom elevation above MSL.

viving high rates of SLR. Such a consideration is directly illustrated in Figure 12. Indeed, relating the higher elevations of the hypsometric curves to the seaward part of the domain and, omitting the channel discontinuities, the lower ones to the landward part, these hypsometric curves may represent the marsh seaward - landward transect, which appears steeper with higher rates of SLR. Since an increase in sedimentation seaward with respect to landward typically leads to a morphological profile that becomes steeper, an equilibrium profile is one where the topographic gradient is low. Therefore, the steeper the profile is, the less resilient the marsh is to rising sea-level, and even if the vegetation attempts to somehow flatten this profile, it is insufficient under high projections of SLR. Likewise, this landward sloping topographic profile can be discerned in some natural salt marshes (see Figure 4a).

As the primary target of the present contribution is to study the influence of SLR on the spatial variation of sedimentation considering different scenarios of colonization by halophytes, the model ingredients necessary to conduct such a detailed investigation involve the use of an "explicit reductionist" (or bottom-up) modeling approach [60], at the expense of relatively costly computational efforts. Therefore, we did not aim to undertake any predictive study but only to appreciate the significance of these spatial dynamics in the context of marsh adaptability with rising sea level. The general idea that marshes must become more inundated before they can accrete at faster rates than that of SLR [59] suggests that perhaps marshes forced by moderate to high SLR scenarios, i.e., $R > 5$ mm/yr, still lag behind the corresponding SLR rates after 60 years, and important changes in marsh behavior may still arise over the longer term [58]. However, the asymptotic trends discerned in Figure 13b denote a progressively slower accretion rate in time for all ecological scenarios which may presage a future stability regime even under high R values.

The threshold R values for marsh survival determined by Kirwan et al. [28] on the basis of the ensemble of numerical models, and later supported by the analytical solution provided by D'Alpaos et al. [17], show that marshes forced by a low microtidal range $2H \leq 1$ m and sediment supply $C = 50$ mg/l should be able to withstand a rate of SLR $R \sim 10$ mm/yr. At first sight, this result seems to contradict our findings. Yet, the difference in the modeling approaches false the comparison. The models used by Kirwan et al. [28] are all point models parameterized with a constant sediment supply C whereas in our 2D approach, $C = 50$ mg/l is imposed at the seaward limit of the domain but, within the marsh, the concentration varies both in time and space as a result of advection/dispersion processes (see Figure 9). Looking at Figure 9, the SSC clearly reduces landward so that defining an equivalent concentration C for the entire lagoon would be, no doubt, lower than 50 mg/l. Therefore, the comparison with results by Kirwan et al. [28] and D'Alpaos et al. [17] must consider marshes characterized by a sediment supply $C < 50$ mg/l, which are indeed able to face a SLR rate $R < 10$ mm/yr, thus in agreement with our simulated marsh

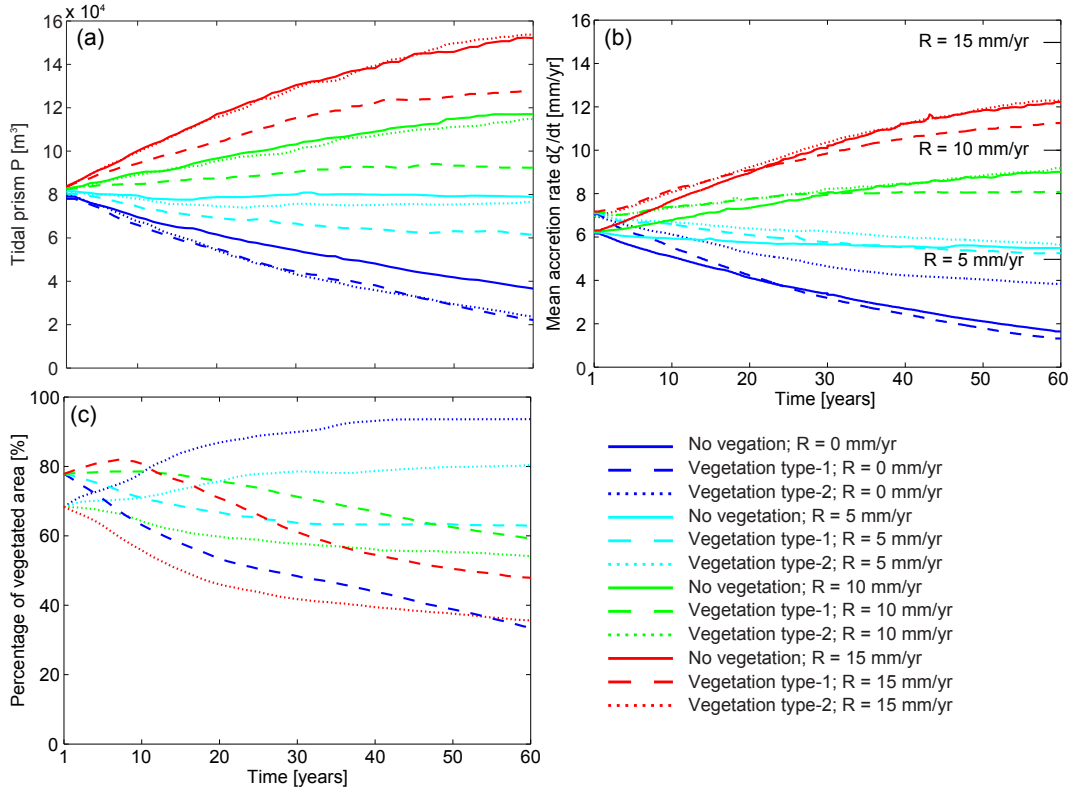

Figure 13: Time series of (a) tidal prism, (b) mean accretion rate and (c) percentage of vegetated area for every SLR and ecological scenario. (For interpretation of the references to colour in this figure text, the reader is referred to the web version of this article).

morphologies obtained imposing a constant value of $C = 50$ mg/l at the seaward limit of the domain.

5. Conclusions

We conducted a conceptual study which aimed to gain further knowledge on the spatial dynamic response of marsh systems in the face of SLR under microtidal conditions and considering different ecological scenarios. The analysis revealed that SLR chiefly controls the global morphological response of the marsh whereas vegetation and its related ecogeomorphic effects on overall showed to be of lesser importance, especially for faster SLR scenarios. Indeed, the tendency put forth by previous field and modeling studies for marshes to persist under conservative projections of SLR and deepen under faster scenarios, which presage their submergence, also holds in the present analysis regardless of the ecological scenarios.

Importantly, this investigation provides insights into the spatial variations of these elevation trajectories. In particular, what appears key for marsh survival is how effective is the transport of sediments toward the inner portions of the marsh that are sediment deficient. Under low SLR scenarios, the largest fraction of the tidal prism is contained in the tidal channels and flows, together with the suspended sediments, towards the inner marsh which in turn experiences significant tidal inundation and sediment deposition, enabling it to accrete and maintain its position in the tidal frame.

Under faster SLR scenarios, the marsh platform globally lowers within the tidal frame, and the resulting greater overmarsh tidal flow in the seaward region triggers an increase in the proportion of SSC that settles down in the seaward marsh platform flanking the tidal channels, whereas a reduced proportion migrates towards the marsh interior. Consequently, the marsh develops a steeper topographic profile where the seaward marsh region accretes at a rate equal to the rate of SLR while the landward marsh, which lacks material, lags behind the rising sea-level. The latter region progressively drowns and the marsh shrinks towards its seaward boundary where the supply of sediment comes from.

Therefore, despite an increase in the rate of SLR draws an increase in the sediment supply in our model, and thus in the total accretion rate across the domain, the analysis has pointed out that beyond sediment availability, its spatial distribution appears to be equally decisive for the assessment of marsh persistence in the face of SLR.

Marshes grown by multiple halophytic communities develop vegetated levees which reduce seaward channel overmarsh flows. Such a behavior associated with the added flow resistance due to plant drag further constrain tidal flows to the channels, thus promoting a greater landward sediment transport towards the inner marsh. Through time, the infilling of this region enables plants to establish which enhances marsh sedimentation, thus raising surface elevation eventually. Yet, with higher SLR projections, the observed die-back of multi-species vegetation limits plant influence on spatial sediment dynamics.

Due to its high productivity at lower elevations, monospecific vegetation typically grows in the low-lying marsh interior, thus supporting marsh sedimentation, but does not colonize the high elevated channel levees on the other hand. This precludes the vegetation-enhanced modulation of channel cross-sections that produces a strong effect on how much sediment can be advected in the channels and therefore distributed on the inner marsh. However, with faster SLR, the progressive marsh platform deepening in the tidal frame triggers plant migration towards the channel levees, allowing monospecific plants in turn to act as a more effective indirect "conveyer" of tidal waters and SSC toward the inner marsh compared to its multi-species counterpart.

Despite SLR outweighs vegetation effects under high projections, this contribution has exposed a series of dynamic and interacting processes by which plants participate and promote the accretion of the marsh surface in ways that increase the resilience of such ecosystems in the context of SLR. This description of the spatial dynamics of marsh systems has thus revealed additional complexities which should need to be considered when addressing the fate of tidal wetlands and their possible restoration in today's changing climate.

Acknowledgments

This work has been carried out within the SMART Joint Doctorate (Science for MAnagement of Rivers and their Tidal Systems), funded with the support of the Erasmus Mundus programme of the European Union, as well as within the 2013 University of Padova project (CPDA133253/13). We also gratefully recognize the contributions of the Editor and the three Reviewers that allowed us to refine the manuscript effectively.

References

[1] S. Temmerman, P. Meire, T. J. Bouma, P. M. Herman, T. Ysebaert, H. J. De Vriend, Ecosystem-based coastal defence in the face of global change, Nature 504 (2013) 79–83.

[2] I. Möller, M. Kudella, F. Rupprecht, T. Spencer, M. Paul, B. K. van Wesenbeeck, G. Wolters, K. Jensen, T. J. Bouma, M. Miranda-Lange, S. Schimmels, Wave attenuation over coastal salt marshes under storm surge conditions, Nature Geoscience 7 (2014) 727–731.

[3] R. Costanza, R. d'Arge, R. De Groot, S. Farber, M. Grasso, B. Hannon, K. Limburg, S. Naeem, R. V. O'Neill, J. Paruelo, R. J. Raskin, P. Sutton, M. van den Belt, The value of the world's ecosystem services and natural capital, Nature 387 (1997).

[4] M. L. Kirwan, J. P. Megonigal, Tidal wetland stability in the face of human impacts and sea-level rise, Nature 504 (2013) 53–60.

[5] C. Craft, J. Clough, J. Ehman, S. Joye, R. Park, S. Pennings, H. Guo, M. Machmuller, Forecasting the effects of accelerated sea-level rise on tidal marsh ecosystem services, Frontiers in Ecology and the Environment 7 (2009) 73–78.

[6] M. Kirwan, S. Temmerman, Coastal marsh response to historical and future sea-level acceleration, Quaternary Science Reviews 28 (2009) 1801–1808.

[7] S. Fagherazzi, M. L. Kirwan, S. M. Mudd, G. R. Guntenspergen, S. Temmerman, A. D'Alpaos, J. Koppel, J. M. Rybczyk, E. Reyes, C. Craft, J. Clough, Numerical models of salt marsh evolution: Ecological, geomorphic, and climatic factors, Reviews of Geophysics 50 (2012).

[8] R. B. Krone, A method for simulating historic marsh elevations, in: Coastal Sediments (1987), ASCE, 1987, pp. 316–323.

[9] J. R. L. Allen, Salt-marsh growth and stratification: a numerical model with special reference to the Severn Estuary, southwest Britain, Marine Geology 95 (1990) 77–96.

[10] J. R. French, Numerical simulation of vertical marsh growth and adjustment to accelerated sea-level rise, north Norfolk, UK, Earth Surface Processes and Landforms 18 (1993) 63–81.

[11] C. Marion, E. J. Anthony, A. Trentesaux, Short-term (≤ 2 yrs) estuarine mudflat and saltmarsh sedimentation: High-resolution data from ultrasonic altimetery, rod surface-elevation table, and filter traps, Estuarine, Coastal and Shelf Science 83 (2009) 475–484.

[12] J. T. Morris, P. V. Sundareshwar, C. T. Nietch, B. Kjerfve, D. R. Cahoon, Responses of coastal wetlands to rising sea level, Ecology 83 (2002) 2869–2877.

[13] S. Temmerman, G. Govers, S. Wartel, P. Meire, Spatial and temporal factors controlling short-term sedimentation in a salt and freshwater tidal marsh, Scheldt estuary, Belgium, SW Netherlands, Earth Surface Processes and Landforms 28 (2003) 739–755.

[14] M. Marani, A. D'Alpaos, S. Lanzoni, L. Carniello, A. Rinaldo, Biologically-controlled multiple equilibria of tidal landforms and the fate of the Venice lagoon, Geophysical Research Letters 34 (2007).

[15] S. M. Mudd, S. M. Howell, J. T. Morris, Impact of dynamic feedbacks between sedimentation, sea-level rise, and biomass production on near-surface marsh stratigraphy and carbon accumulation, Estuarine, Coastal and Shelf Science 82 (2009) 377–389.

[16] L. G. Larsen, J. W. Harvey, How vegetation and sediment transport feedbacks drive landscape change in the everglades and wetlands worldwide, American Naturalist 176 (2010) E66–E79.

[17] A. D'Alpaos, S. M. Mudd, L. Carniello, Dynamic response of marshes to perturbations in suspended sediment concentrations and rates of relative sea level rise, Journal of Geophysical Research: Earth Surface 116 (2011).

[18] M. L. Kirwan, A. B. Murray, A coupled geomorphic and ecological model of tidal marsh evolution, Proceedings of the National Academy of Sciences 104 (2007) 6118–6122.

[19] C. T. Friedrichs, J. E. Perry, Tidal salt marsh morphodynamics, Journal of Coastal Research 27 (2001) 6–36.

[20] M. Marani, C. Da Lio, A. DAlpaos, Vegetation engineers marsh morphology through multiple competing stable states, Proceedings of the National Academy of Sciences 110 (2013) 3259–3263.

[21] A. D'Alpaos, The mutual influence of biotic and abiotic components on the long-term ecomorphodynamic evolution of salt-marsh ecosystems, Geomorphology 126 (2011) 269–278.

[22] S. M. Mudd, S. Fagherazzi, J. T. Morris, D. J. Furbish, Flow, sedimentation, and biomass production on a vegetated salt marsh in south carolina: Toward a predictive model of marsh morphologic and ecologic evolution, in: S. Fagherazzi, A. Marani, L. K. Blum (Eds.), The Ecogeomorphology of Tidal Marshes, Coastal and Estuarine Stud, 2004, pp. 165–188.

[23] C. Da Lio, A. D'Alpaos, M. Marani, The secret gardener: Vegetation and the emergence of biogeomorphic patterns in tidal environments, Philosophical Transactions of the Royal Society A: Mathematical, Physical and Engineering Sciences 371 (2013).

[24] A. Rinaldo, S. Fagherazzi, S. Lanzoni, M. Marani, W. E. Dietrich, Tidal networks: 2. watershed delineation and comparative network morphology, Water Resources Research 35 (1999) 3905–3917.

[25] A. D'Alpaos, S. Lanzoni, M. Marani, A. Rinaldo, Landscape evolution in tidal embayments: Modeling the interplay of erosion, sedimentation, and vegetation dynamics, Journal of Geophysical Research: Earth Surface 112 (2007).

[26] J.-P. Belliard, M. Toffolon, L. Carniello, A. D'Alpaos, An ecogeomorphic model of tidal channel initiation and elaboration in progressive marsh accretional contexts, Journal of Geophysical Research: Earth Surface 120 (2015) 1040–1064.

[27] D. J. Reed, The response of coastal marshes to sea-level rise: Survival or submergence?, Earth Surface Processes and Landforms 20 (1995) 39–48.

[28] M. L. Kirwan, G. R. Guntenspergen, A. D'Alpaos, J. T. Morris, S. M. Mudd, S. Temmerman, Limits on the adaptability of coastal marshes to rising sea level, Geophysical Research Letters 37 (2010).

[29] A. Defina, Two-dimensional shallow flow equations for partially dry areas, Water Resources Research 36 (2000) 3251–3264.

[30] L. Carniello, A. Defina, S. Fagherazzi, L. D'alpaos, A combined wind wave–tidal model for the Venice Lagoon, Italy, Journal of Geophysical

Research 110 (2005).
[31] L. Carniello, A. DAlpaos, A. Defina, Modeling wind waves and tidal flows in shallow micro-tidal basins, Estuarine, Coastal and Shelf Science 92 (2011) 263–276.
[32] L. Carniello, S. Silvestri, M. Marani, A. D'Alpaos, V. Volpe, A. Defina, Sediment dynamics in shallow tidal basins: In situ observations, satellite retrievals, and numerical modeling in the Venice Lagoon, Journal of Geophysical Research 119 (2010) 802–815.
[33] L. Carniello, A. Defina, L. DAlpaos, Modeling sand-mud transport induced by tidal currents and wind waves in shallow microtidal basins: Application to the Venice Lagoon (Italy), Estuarine, Coastal and Shelf Science 102 (2012) 105–115.
[34] E. Partheniades, Erosion and deposition of cohesive soils, Journal of the Hydraulics Division, ASCE 91 (1965) 105–139.
[35] R. B. Krone, Flume studies of the transport of sediment in estuarial shoaling processes, Technical Report, Hydr, Eng. Laboratory, Univ of Berkely, USA, 1962.
[36] J. A. Roelvink, Coastal morphodynamic evolution techniques, Coastal Engineering 53 (2006) 277–287.
[37] M. R. Palmer, H. M. Nepf, T. J. R. Pettersson, J. D. Ackerman, Observations of particle capture on a cylindrical collector: Implications for particle accumulation and removal in aquatic systems, Limnology and Oceanography 49 (2004) 76–85.
[38] G. Coco, Z. Zhou, B. van Maanen, M. Olabarrieta, R. Tinoco, I. Townend, Morphodynamics of tidal networks: Advances and challenges, Marine Geology 346 (2013) 1–16.
[39] G. Caniglia, G. Contin, M. Fusco, N. Anoé, A. Zanaboni, Confronto su base vegetazionale tra due barene della laguna di venezia, Fitosociologia 34 (1997) 111–119.
[40] J. T. Morris, D. Porter, M. Neet, P. A. Noble, L. Schmidt, L. A. Lapine, J. R. Jensen, Integrating LIDAR elevation data, multi-spectral imagery and neural network modelling for marsh characterization, International Journal of Remote Sensing 26 (2005) 5221–5234.
[41] S. Silvestri, A. Defina, M. Marani, Tidal regime, salinity and salt marsh plant zonation, Estuarine, Coastal and Shelf Science 62 (2005) 119–130.
[42] R. Torres, R. Styles, Effects of topographic structure on salt marsh currents, Journal of Geophysical Research: Earth Surface (2003–2012) 112 (2007).
[43] M. Marani, S. Lanzoni, S. Silvestri, A. Rinaldo, Tidal landforms, patterns of halophytic vegetation and the fate of the lagoon of Venice, Journal of Marine Systems 51 (2004) 191–210.
[44] P. F. Randerson, A simulation model of salt-marsh development and plant ecology, in: Estuarine and coastal land reclamation and water storage, Saxon House, Farnborough, 1979, pp. 48–67.
[45] T. Christiansen, P. L. Wiberg, T. G. Milligan, Flow and sediment transport on a tidal salt marsh surface, Estuarine, Coastal and Shelf Science 50 (2000) 315–331.
[46] N. L. Bindoff, J. Willebrand, V. Artale, A. Cazenave, J. Gregory, S. Gulev, K. Hanawa, C. Le Quéré, S. Levitus, Y. Nojiri, C. K. Shum, T. L. D., A. Unnikrishnan, Observations: oceanic climate change and sea level, in: S. Solomon, D. Qin, M. Manning, Z. Chen, M. Marquis, K. Averyt, M. Tignor, H. Miller (Eds.), Climate Change 2007: The Physical Science Basis: Contribution of Working Group I to the Fourth Assessment Report of the Intergovernmental Panel on Climate Change, Cambridge University Press, Cambridge, UK and New York, NY, USA, 2007, pp. 385–433.
[47] S. Temmerman, T. J. Bouma, G. Govers, D. Lauwaet, Flow paths of water and sediment in a tidal marsh: Relations with marsh developmental stage and tidal inundation height, Estuaries 28 (2005) 338–352.
[48] S. Rahmstorf, A semi-empirical approach to projecting future sea-level rise, Science 315 (2007) 368–370.
[49] T. Bayliss-Smith, R. Healey, R. Lailey, T. Spencer, D. R. Stoddart, Tidal flows in salt marsh creeks, Estuarine and Coastal Marine Science 9 (1979) 235–255.
[50] J. R. French, D. R. Stoddart, Hydrodynamics of salt marsh creek systems: Implications for marsh morphological development and material exchange, Earth surface processes and landforms 17 (1992) 235–252.
[51] A. D'Alpaos, S. Lanzoni, S. M. Mudd, S. Fagherazzi, Modeling the influence of hydroperiod and vegetation on the cross-sectional formation of tidal channels, Estuarine, Coastal and Shelf Science 69 (2006) 311–324.
[52] J. R. L. Allen, Morphodynamics of Holocene salt marshes: a review sketch from the Atlantic and Southern North Sea coasts of Europe, Quaternary Science Reviews 19 (2000) 1155–1231.
[53] S. Fagherazzi, M. Hannion, P. D'Odorico, Geomorphic structure of tidal hydrodynamics in salt marsh creeks, Water resources research 44 (2008).
[54] Z. J. Hughes, Tidal channels on tidal flats and marshes, in: R. A. J. Davis, R. W. Dalrymple (Eds.), Principles of Tidal Sedimentology, 2012, pp. 269–300.
[55] B. Van Maanen, G. Coco, K. R. Bryan, C. T. Friedrichs, Modeling the morphodynamic response of tidal embayments to sea-level rise, Ocean Dynamics 63 (2013) 1249–1262.
[56] J. P. Donnelly, M. D. Bertness, Rapid shoreward encroachment of salt marsh cordgrass in response to accelerated sea-level rise, Proceedings of the National Academy of Sciences 98 (2001) 14218–14223.
[57] J. S. Pethick, Long-term accretion rates on tidal salt marshes, Journal of Sedimentary petrology 51 (1981) 571–577.
[58] M. L. Kirwan, A. B. Murray, Tidal marshes as disequilibrium landscapes? Lags between morphology and Holocene sea level change, Geophysical Research Letters 35 (2008).
[59] J. R. French, Tidal marsh sedimentation and resilience to environmental change: exploratory modelling of tidal, sea-level and sediment supply forcing in predominantly allochthonous systems, Marine Geology 235 (2006) 119–136.
[60] A. B. Murray, Contrasting the goals, strategies, and predictions associated with simplified numerical models and detailed simulations, in: Prediction in geomorphology, 2003, pp. 151–165. doi:10.1029/135GM11.